Evaporative Cooling of Antiprotons for the Production of Trappable Antihydrogen

D. M. Silveira[*], M. D. Ashkezari[†], M. Baquero-Ruiz[**], W. Bertsche[‡,§], E. Butler[¶], C. L. Cesar[*], M. Charlton[‖], J. Fajans[**], T. Friesen[††], M. C. Fujiwara[‡‡], D. R. Gill[‡‡], J. S. Hangst[§§], W. N. Hardy[¶¶], M. E. Hayden[†], S. Jonsell[***], L. Kurchaninov[‡‡], N. Madsen[‖], S. Menary[†††], P. Nolan[‡‡‡], K. Olchansky[‡‡], A. Olin[‡‡], A. Povilus[**], P. Pusa[‡‡‡], F. Robicheaux[§§§], E. Sarid[¶¶¶], C. So[**], R. I. Thompson[††], D. P. van der Werf[‖] and J. S. Wurtele[**]

[*]*Instituto de Física - Universidade Federal do Rio de Janeiro, 21941-972, Rio de Janeiro, Brazil*
[†]*Department of Physics, Simon Fraser University, Burnaby BC, V5A 1S6, Canada*
[**]*Department of Physics, University of California, Berkeley, California 94720-7300, USA*
[‡]*School of Physics and Astronomy, University of Manchester, M13 9PL Manchester, UK*
[§]*The Cockroft Institute, WA4 4AD Warrington, UK*
[¶]*CERN, PH Department, CH-1211 Geneva 23, Switzerland*
[‖]*Department of Physics, Swansea University, Swansea SA2 8PP, UK*
[††]*Department of Physics and Astronomy, University of Calgary AB, T2N 1N4, Canada*
[‡‡]*TRIUMF, 4004 Wesbrook Mall, Vancouver BC, V6T 2A3, Canada*
[§§]*Department of Physics and Astronomy, Aarhus University, DK-8000 Aarhus C, Denmark*
[¶¶]*Department of Physics and Astronomy, University of British Columbia, Vancouver BC, V6T 2A3, Canada*
[***]*Department of Physics, Stockholm University, SE-10691 Stockholm, Sweden*
[†††]*Department of Physics and Astronomy, York University, Toronto ON, M3J 1P3, Canada*
[‡‡‡]*Department of Physics, University of Liverpool, Liverpool L69 7ZE, UK*
[§§§]*Department of Physics, Auburn University, Auburn, Alabama 36849-5311, USA*
[¶¶¶]*Department of Physics, NRCN - Nuclear Research Center Negev, Beer Sheva, IL - 84190, Israel*

Abstract.
We describe the implementation of evaporative cooling of charged particles in the ALPHA apparatus. Forced evaporation has been applied to cold samples of antiprotons held in Malmberg-Penning traps. Temperatures on the order of 10 K were obtained, while retaining a significant fraction of the initial number of particles. We have developed a model for the evaporation process based on simple rate equations and applied it succesfully to the experimental data. We have also observed radial redistribution of the clouds following evaporation, explained by simple conservation laws. We discuss the relevance of this technique for the recent demonstration of magnetic trapping of antihydrogen.

Keywords: Antihydrogen, evaporative cooling, Penning trap
PACS: 36.10.-k, 52.27.Jt, 52.20.Hv

INTRODUCTION

Evaporative cooling is a powerful technique for reducing the temperature of an ensemble of particles bound to a finite-depth potential well. Cooling is obtained by selectively removing the most energetic particles from a thermal distribution and allowing the resulting energy reduction to be shared by all the remaining particles. It was originally proposed [1] and demonstrated [2] for atomic hydrogen, but its use became widespread

after being successfully used for the production of Bose-Einstein condensates of alkali-atom samples [3]. More than 15 years after that, evaporative cooling remains a mandatory last step for the observation of condensates and became an ubiquitous technique in neutral atom and molecule trapping. But despite its extensive use in cold atom experiments, evaporation has found a very limited application for charged particles: it has been applied to highly charged ions in EBITs at energies around 100 eV [4].

In this paper, we report evaporative cooling of charged particles in Malmberg-Penning traps. These traps are part of the ALPHA apparatus, an experimental system which was recently used to demonstrate for the first time the confinement of antihydrogen atoms in a magnetic trap [5]. The main goal of the ALPHA experiment is to perform a sensitive test of CPT symmetry [6], through a direct spectroscopic comparison between antihydrogen and its matter counterpart (atomic hydrogen). It is likely that the ultimate precision in this measurement can only be reached in a magnetic trap [7]. In our system, antihydrogen is produced [8] by merging cold clouds of its constituents (antiprotons and positrons) confined by the electric and magnetic fields of a Malmberg-Penning trap. With a magnetic trap superposed to the charged particle traps, the fraction of antihydrogen atoms produced with a kinetic energy lower than the (magnetic) well depth will be initially confined. From the spectroscopy point of view, it is certainly interesting to increase this trappable fraction as much as possible, given the expected gain in signal-to-noise ratio.

The current technology and our experimental constraints (especially those related to our annihilation detection scheme) limit the available well depth to ~ 1 T, which corresponds to antihydrogen with a maximum kinetic energy of ~ 0.7 K. The conclusion is that the anti-atoms have to be cold in order to be captured by the magnetic trap. One of the routes to increase the trappable (i.e., cold) fraction of the synthesized anti-atoms is to keep the temperatures of both charged species as low as possible until the moment they recombine. With the two oppositely-charged charged species trapped in neighboring potential wells of the Malmberg-Penning trap (the so-called nested-trap scheme [9]), recombination can be initiated by sending one species through the other. The kinetic energy of antihydrogen is mainly set by the kinetic energy of the antiproton; for recombination schemes in which the antiproton cloud is held stationary as it is traversed by the positrons (or by the positron-containing species, such as positronium atoms), a lower antiproton temperature will result in a larger number of trappable antihydrogen atoms. For schemes in which antiprotons are sent into the positron cloud the relation is not so obvious, as the energy given to the former also has to be taken into account.

The renowned cooling procedure for antiprotons is collisional de-excitation by electrons [10]. The main advantage is that electron cooling is already required to capture the antiproton bunch from the Antiproton Decelerator: a pre-loaded electron plasma is used to cool antiprotons from the initial capture energy of 5 keV to much lower energies. The energy exchanged with the electrons is radiated away as cyclotron radiation and after some time both species should reach thermal equilibrium. The ultimate limit for this equilibrium temperature is given by the radiative exchange between electrons and the cold surfaces of the trap and, in a simplified analysis, the mixed antiproton-electron plasma should reach the same temperature as the trap electrodes. But in our traps the observed electron plasma temperatures are at least 10 - 20 times the electrode temper-

ature. In conclusion, electron cooling is very efficient in cooling antiprotons from keV energies to tens of meV, but it fails in providing a cold sample of antiprotons. But even if electron cooling worked as initially expected, one would be still left with the problem of electron removal. The presence of electrons during recombination can be a nuisance: they can deplete the positron cloud (through positronium formation) or partially neutralize it (leading to destabilization), or simply destroy the antihydrogen atoms by charge exchange reactions. Our current procedure for electron ejection involves pulsed fields and, while working very efficiently, it leaves antiproton samples with temperatures no lower than 200 - 300 K.

A final motivation for antiproton cooling is related to the particular technique we employ to drive the antiprotons into the positron plasma: the autoresonant frequency sweep has been shown to work more efficiently when the antiprotons are colder [11]. At lower temperatures, the whole sample behaves as a single-particle nonlinear oscillator and can be entirely excited to be brought into contact with the positron plasma.

EVAPORATIVE COOLING OF NEUTRAL AND CHARGED PARTICLES

Elastic collisions are the driving force behind evaporative cooling, continuously providing particles with energy above the well depth. Furthermore, for evaporation to work as a cooling process the energy deficit resulting from the escaping particles has to be re-distributed, a process which is also driven by elastic collisions. As a result of the long range nature of the Coulomb interaction, typical collision rates are very high. Thus, for comparable values of densities and temperatures, samples of charged particles constitute a much better system for the implementation of evaporation than clouds of neutral particles. And as evaporation progresses, the increase in the collision frequency with decreasing energy ensures a sustained efficiency for cooling of trapped charged samples. This means that manipulations normally used to increase the collision frequency in atom traps (such as adiabatic compression [12]) will not be required in Malmberg-Penning traps. A third advantage for charged particles is the absence of intra-species trap-loss channels (like spin-exchange and inelastic dipolar collisions, in the case of neutral particles [13]) which could compete with the cooling power available from evaporation. On the other hand, the absence of these trap loss channels precludes an energy-selective removal of particles through transitions to untrapped states, like in rf evaporation of neutral particles [14].

The simplest implementation of evaporative cooling in magnetic traps involves slowly ramping down the confining magnetic field. In a Malmberg-Penning trap radial confinement is provided by a solenoidal magnetic field and axial confinement is maintained by electrostatic potentials applied to the cylindrical electrodes. With this arrangement, evaporation can be achieved by slowly lowering one of the side walls of the axial well. Strictly speaking, this implementation also means that evaporation is 1D because the escape criterion is $\varepsilon_z > \varepsilon_T$. But the high collision rate guarantees an extremely fast anisotropic relaxation rate and, in practice, a 3D evaporation. Here the z-axis is the trap axis and ε_T is the axial well depth. The strong coupling between elementary charges and typical trapping electrical fields (much larger than the coupling between atomic dipole

moments and typical trapping magnetic fields) requires a much more precise control of the confining voltages during evaporation: this is certainly the major technical challenge for the efficient use of evaporation with charged particles.

Another peculiarity of this implementation of evaporation is that our charged particle samples are in the plasma regime. The electric fields from the charge distribution itself (space charge potentials) can be comparable to the 'vacuum' fields produced by the electrodes and, as a result of the coupling between them, the effective well depth seen by the trapped particles will be reduced.

EXPERIMENTAL PROCEDURE

A schematic view of the ALPHA apparatus is depicted in Fig. 1(a), showing only the relevant parts for the evaporation measurements. The cylindrical electrode stack is placed inside a vacuum chamber, whose outer surface is cooled by a liquid helium bath; the electrodes reach a temperature around 7 K. The devices on either end of the vacuum tube are used for diagnostics of the charged particles. On the left, a thin aluminum foil (used as the final degrading material when the antiproton bunch enters the trap) is used as a Faraday cup. On the right, a combined micro-channel plate and phosphor screen assembly (MCP/Phosphor) allows the measurement of the clouds spatial density profile (integrated along the z-axis) [15]. The trap is immersed in the uniform 1 T field of an external superconducting solenoid, which is kept constant throughout the measurements. Externally to the solenoid, a set of plastic scintillators read out by photomultiplier tubes is used to detect the products of antiproton annihilations.

For a full characterization of the evaporation process, one is interested in measuring the temperature and the number of remaining particles after the evaporation ramp. The number of antiprotons can be measured by allowing the particles to escape from the well towards the aluminum foil, where they annihilate. The annihilation products are then detected by the scintillators with an efficiency of $(25 \pm 10)\%$ per event. To measure the plasma temperatures, we employed a simplified version of the parallel-temperature diagnostic [16], where a Maxwell-Boltzmann distribution is fit to the high-energy tail of the energy distribution. This distribution is measured by slowly letting the particles escape from the axial electrostatic well towards the aluminum foil. The time-resolved signal measured at the detectors is then mapped to the original well, giving the energy distribution the particles had before the potentials were changed for the measurement. In our procedure, the number of antiprotons and their temperature are simultaneously measured by allowing all the particles remaining after evaporation to escape: the fit to the high-energy portion of the distribution gives the temperature, while the total number of particles detected during the manipulation gives the particle number.

The temperature values obtained from the fits have been corrected by a numerical factor determined by a particle-in-cell (PIC) simulation of the particle escape from the potential well. The computer simulation include effects that happen during the potential manipulation which could result in a measured temperature different from the temperature the plasma had before the measurement started: the time evolution of the vacuum and space charge potentials, the possibility of evaporative cooling and the energy exchange between the different translational degrees of freedom. The result
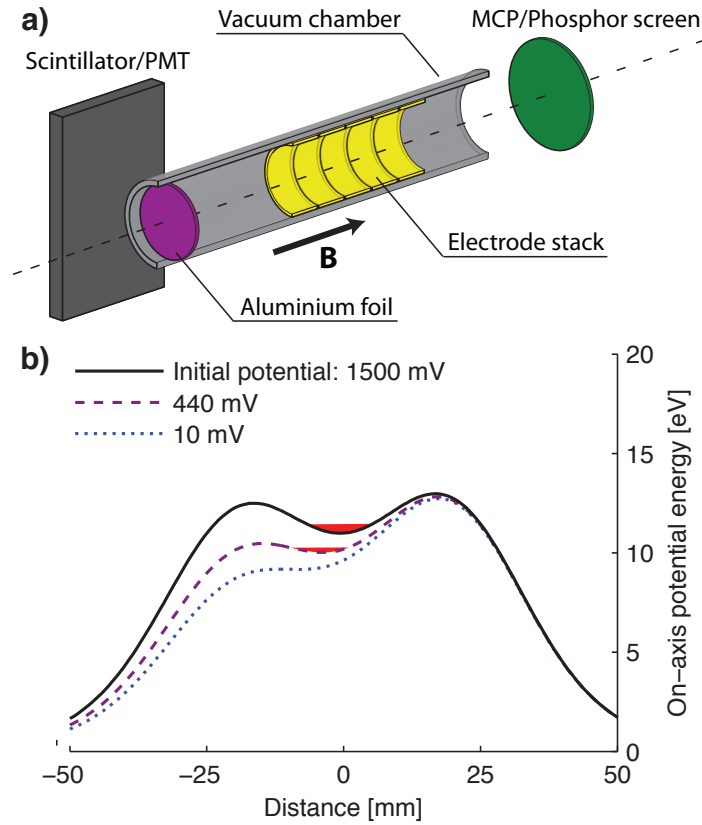
FIGURE 1. (a) Simplified schematic view of the ALPHA apparatus, showing the trap electrodes and the 2 devices used to characterize the evaporation process. (b) Some of the potential wells used for the experiments: the initial well (1500 mV), the deepest (440 mV) and the shallowest (10 mV) wells

is that the measured temperatures are $\sim 16\%$ higher than the true temperatures; all temperatures reported here have been corrected accordingly.

In addition to the temperature and number measurement, the radial profile after evaporation can be measured by ejecting the particles towards the MCP/Phosphor. This gives complementary information about the evaporation process.

EVAPORATIVE COOLING OF ANTIPROTONS

We initially prepare a sample of 45000 antiprotons with a density of $7.5 \times 10^6 cm^{-3}$ in a cloud with a 0.6 mm radius. Details about the preparation of these clouds can be found in [17]. The antiprotons are initially confined in a 1500 mV-deep well (on-axis well depth), with a temperature of (1040 ± 45) K. Forced evaporative cooling is performed by linearly ramping the voltage applied to one of the confining electrodes that produces the confining well. The original 1500 mV well is ramped to six previously chosen wells, with on-axis depths ranging from 440 mV to 10 mV (Fig. 1(b)). The particles are then allowed to reequilibrate for 10 s before a measurement (either number/temperature or radial profile) is made. Note that evaporation is initiated by lowering one of the sides
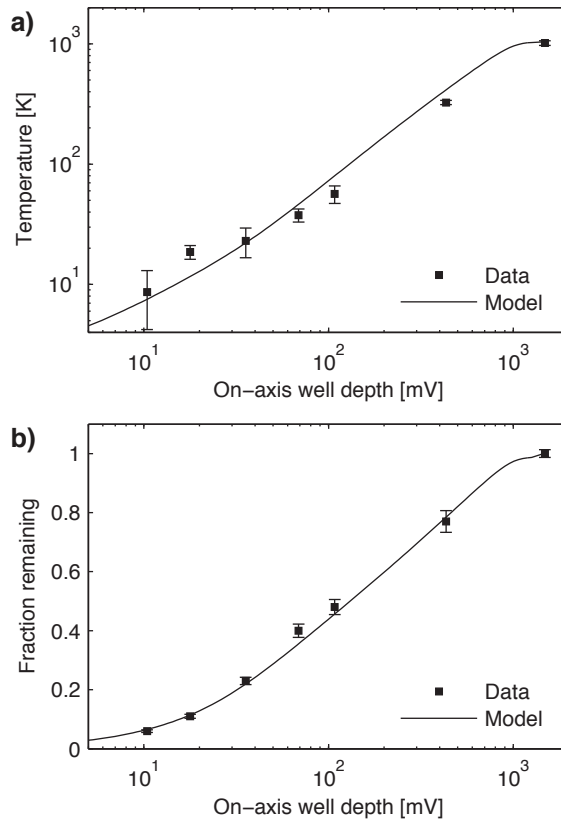
FIGURE 2. (a) Temperature as a function of the on-axis well depth: the points are measured temperatures. (b) Remaining fraction as a function of the on-axis well depth: the points are measured fractions. In both graphs the line is the result of the model.

of the confining well; since the aluminum foil and the MCP/phosphor are at opposite ends of the trap, for the radial profile measurement the well has to be changed so that the lower wall is to the right of the plasma (see Fig. 1(b) for reference). But other than that, the wells are absolutely equal.

In Figure 2(a) the temperature for each of the 6 wells is shown as a function of the well depth in a log-log plot; the temperature and well depth before evaporation are also displayed. From the initial temperature of 1040 K, temperatures between 9 and 325 K can be obtained. The remaining fraction for each of the wells as a function of the well depth is shown in Fig. 2(b), together with the initial fraction. Depending on the well depth, the number of particles is reduced from 45000 to fractions between 6% and 77%.

For the data presented in Fig. 2, the evaporation ramps were 100 s long, but we investigated different ramp times (300, 30, 10 and 1 s) with very similar results. The only exception was the 1 s ramp, for which we observed much lower remaining fractions for all well depths; in particular for the 10 mV well, less than 0.1% of the initial number was left at the end.
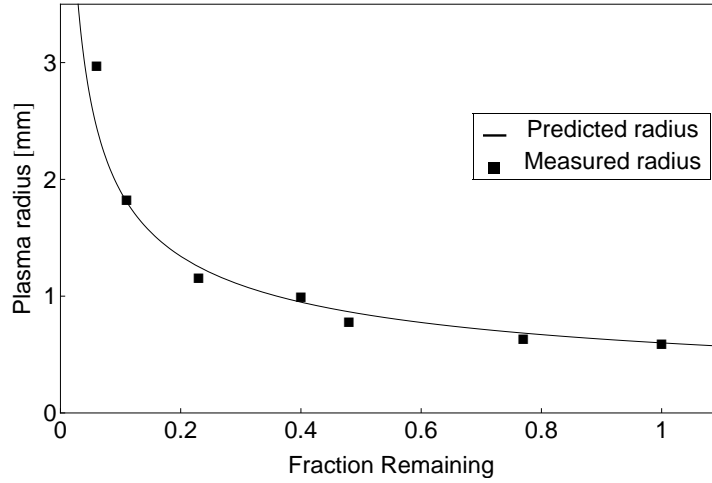
FIGURE 3. Plasma radius after evaporation ramp as a function of the remaining fraction. Points are experimental data, line is the prediction from Eq. 2

For each of the radial profile measurements, a 2D gaussian profile of the type

$$f(x,y) = A \exp\left[-\frac{(x-x_0)^2 + (y-y_0)^2}{b^2}\right] + C \tag{1}$$

is fitted, and the plasma radius (b) is obtained. This data shows an increase in b with decreasing well depth: from the initial value of 0.6 mm, the radius grows to 3 mm (for the shallowest well). In a Malmberg-Penning trap evaporation happens preferentially close to the trap axis, where the potential barrier the particles have to overcome is the lowest. If we assume that all evaporating particles escape from the radial center of the cloud, the total canonical angular momentum is conserved and will have to be redistributed among a smaller number of particles. As a consequence, the average radius of the cloud will increase. The total canonical angular momentum is proportional to $\sum r_j^2$, where r_j is the radial location of each particle and the sum is over all particles in the cloud. We can thus obtain a scaling law for the radial expansion, relating the particle number and the cloud mean square radius before and after evaporation:

$$\frac{N_0}{N} = \frac{\langle r^2 \rangle}{\langle r_0^2 \rangle}. \tag{2}$$

In Fig. 3, the cloud radius is shown as a function of the remaining fraction. The line represents the relation predicted by Eq. 2, and shows a good agreement with the measured data. It is important to note that this equation represents an upper limit, as the particles which escape not exactly on axis carry away some angular momentum (proportional to r_j), reducing the amount to be redistributed and the radial expansion.

Evaporative cooling is usually modeled by rate equations describing the time evolution of the number of trapped particles and the temperature [18]. In the case of evaporation of antiprotons in Malmberg-Penning traps, the equations have to be modified to

take into account the particularities of this system. First, a loss term has to be added to account for the annihilation of antiprotons on the background gas in the trap. Second, a heating term must also be added to take into account heating sources. As the cloud expands to conserve angular momentum, Joule heating from the conversion of electrostatic potential energy to kinetic energy will compete with the cooling provided by evaporation. The equations then become

$$\frac{dN}{dt} = -\frac{N}{\tau_{ev}} - \gamma N, \tag{3}$$

$$\frac{dT}{dt} = -\alpha \frac{T}{\tau_{ev}} + P, \tag{4}$$

where τ_{ev} is the evaporation timescale and α represents the efficiency of evaporation (the temperature decrease per particle lost). The loss term γ (1×10^{-4} s^{-1} per particle) is readily obtained, as the detector monitors annihilations during all the stages of the experiment. The heating term P is estimated as $(-dN/dt) \times 5$ mK from a simple model for Joule heating.

The efficiency parameter can be written [18] as

$$\alpha = \frac{\eta + \kappa}{\delta + 3/2} - 1, \tag{5}$$

where η, κ and δ are energy scales relevant to the experiment: η is the well depth (in terms of energy), κ is the excess kinetic energy of an evaporating particle and $\delta + 3/2$ is the sum of kinetic and potential energy (for all three parameters, the energies are given in units of $k_B T$, with k_B being the Boltzmann constant). In our case, we approximate κ by 1 [18] and let $\delta = 1/2$, as this closely describes our well geometry.

The evaporation timescale τ_{ev} is related to the rate at which collisions promote trapped particles to energies above the well depth. In the case of one dimensional evaporation [19] it can be related to the antiproton relaxation time τ_{coll} with

$$\frac{\tau_{ev}}{\tau_{coll}} = \frac{\sqrt{2}}{3} \eta e^{\eta}, \tag{6}$$

In our case, the relevant collision mechanism is the relaxation between the parallel and perpendicular temperatures (parallel and perpendicular refer to the direction of the magnetic field). For τ_{coll}, we use the expression obtained in [20].

With all the parameters appearing in Eqs. 3 and 4 outlined, the time dependency of N and T is obtained by numerically solving these equations. The time dependency is then converted to a well depth dependency and these are the curves plotted in Figs. 2a and 2b. In both graphs, we observe a very good agreement between the model and the experimental data. This shows that our choices of α and P were sound.

EVAPORATION AND THE PRODUCTION OF TRAPPABLE ANTIHYDROGEN

Evaporative cooling reduces the temperature of a trapped sample at the expense of particle number. While this may not be a problem for atom traps initially loaded with 10^{12} atoms, it is certainly a limitation if one plans to cool antiprotons (available in numbers close to 5×10^4 every ~ 100 s). Despite the reduction in particle number, our results represent an increase in the absolute number of antiprotons with energies below the currently-used well depth (0.5 K $\times$ k_B, in energy units): for the lowest temperature observed, this number increases by 2 orders of magnitude.

In ALPHA, antihydrogen is produced by keeping the positron plasma stationary and sending antiprotons through. The integration of antiproton evaporative cooling into such a production scheme isn't straightforward, because the manipulations required to bring the antiprotons into contact with the positrons would certainly heat up the former species. All possible gains obtained by evaporation would then be lost.

At the end of 2009, we started to observe signals in our apparatus compatible with trapped antihydrogen. At that time evaporation wasn't being used, but we were able to observe 6 candidate events in 212 attempts [21]. Early in 2010 we applied our evaporation knowledge to positron clouds, and found out that they can also be efficiently cooled by evaporation (it's important to mention that, like the electron plasmas, our positron samples don't cool to the environment temperature). Implementation of this step in the mixing/trapping sequence was much easier and this technique, together with the development of procedures to rule out the possibility of false positives [5], allowed us to make the first observation of trapped antihydrogen. The number of trapped atoms initially observed was 38 in 335 attempts.

Following developments in the radial compression of trapped species (before the recombination stage) and in the autoresonant injection of antiprotons, we were finally able to integrate antiproton evaporation into the antihydrogen production procedure. Currently all antihydrogen production experiments at ALPHA include evaporative cooling of both charged species.

REFERENCES

1. H. F. Hess, *Phys. Rev. B* **34**, 3476 - 3479 (1986).
2. N. Masuhara, J. M. Doyle, J. C. Sandberg, D. Kleppner, T. J. Greytak, H. F. Hess, and G. P. Kochansky, *Phys. Rev. Lett.* **61**, 935 - 938 (1988).

3. M. H. Anderson, J. R. Ensher, M. R. Matthews, C. E. Wieman, and E. A. Cornell, *Science* **269**, 198 - 201 (1995).
4. T. Kinugawa, F. J. Currell, and S. Ohtani, *Phys. Scr.* **T92**, 102 - 104 (2001).
5. G. B. Andresen *et al.* (ALPHA Collaboration), *Nature* **468**, 673 -676 (1995).
6. G. Lüders, *Ann. Phys.* **2**, 1 - 15 (1957).
7. C. L. Cesar, D. G. Fried, T. C. Killian, A. D. Polcyn, J. C. Sandberg, I. A. Yu, T. J. Greytak, D. Kleppner, and J. M. Doyle, *Phys. Rev. Lett.* **77**, 255 - 258 (1996).
8. G. B. Andresen *et al.* (ALPHA Collaboration), *J. Phys. B: At. Mol. Opt. Phys.* **41**, 011001 (2008).
9. G. Gabrielse, S. L. Rolston, L. Haarsma, and W. Kells, *Phys. Lett. A* **129**, 38 - 42 (1988).
10. G. Gabrielse, X. Fei, L. A. Orozco, R. L. Tjoelker, J. Haas, H. Kalinowsky, T. A. Trainor, and W. Kells, *Phys. Rev. Lett.* **63**, 1360 - 1363 (1989).
11. G. B. Andresen *et al.* (ALPHA Collaboration), *Phys. Rev. Lett.* **106**, 025002 (2011).
12. K. B. Davis, M.-O. Mewes, M. A. Joffe, M. R. Andrews, and W. Ketterle, *Phys. Rev. Lett.* **74**, 5202 - 5205 (1995).
13. A. Lagendjik, I. F. Silvera, B. J. Verhaar, *Phys. Rev. B* **33**, 626 - 628 (1986).
14. D. E. Pritchard, K. Helmerson, and A. G. Martin, "Atom Traps", in *Atomic Physics XI*, edited by S. Haroche, J. C. Gay, and G. Grynberg, World Scientific, Singapore, 1989, pp 179 - 197.
15. G. B. Andresen *et al.* (ALPHA Collaboration), *Rev. Scient. Inst.* **80**, 123701 (2009).
16. D. L. Eggleston, C. F. Driscoll, B. R. Beck, A. W. Hyatt, and J. H. Malmberg, *Phys. Fluids B* **4**, 3432 - 3439 (1992).
17. G. B. Andresen *et al.* (ALPHA Collaboration), *Phys. Rev. Lett.* **105**, 013003 (2010).
18. W. Ketterle and N. J. Van Druten, *Adv. At. Mol. Opt. Phys.* **37**, 181 - 236 (1996).
19. G. Fussmann, C. Biedermann, and R. Radtke, "EBIT: An Electron Beam Source for the Production and Confinement of Highly Ionized Atoms", in *Advanced Technologies Based on Wave and Beam Generated Plasmas*, edited by H. Schlüter and A. Shivarova, Kluwer Academic Publishers, Dordrecht, 1999, pp 429 - 467.
20. M. E. Glinsky, T. M. O'Neil, M. N. Rosenbluth, K. Tsuruta, and S. Ichimaru, *Phys. Fluids B* **4**, 1156 - 1166 (1992).
21. G. B. Andresen *et al.* (ALPHA Collaboration), *Phys. Lett. B* **695**, 95 - 104 (2011).